



KUNGL
TEKNISKA
HÖGSKOLAN

Royal Institute of Technology
Dept. of Numerical Analysis and Computer Science

*PML-methods for the linearized Euler
equations*

by
Daniel Appelö

TRITA-NA-E00XY



NADA

Nada (Numerisk analys och datalogi)
KTH
100 44 Stockholm

Department of Numerical Analysis
and Computer Science
Royal Institute of Technology
SE-100 44 Stockholm, SWEDEN

PML-methods for the linearized Euler equations

by
Daniel Appelö

TRITA-NA-E00XY

Master's Thesis in Numerical Analysis (20 credits)
at the School of Electrical in electrical engineering,
Royal Institute of Technology year 2000
Supervisor at Nada was Gunilla Kreiss
Examiner was Jesper Ooppelstrup

Abstract

A recently suggested method for absorbing boundary conditions for the Euler equations is examined. The method is of PML type and has the important property of being well posed. Results from numerical experiments using a second order discretization are presented. For some choices of parameters the method becomes unstable. The instability is observed to originate from the corner regions. A modification to avoid these instabilities is suggested. The PML method is tested for a variable Mach number problem. The performance does not seem to be degraded. Optimization of parameters in the method is performed.

Contents

1	Introduction	9
2	Theoretical Background	11
2.1	Absorbing boundary conditions	11
2.1.1	Classic analytical ABCs for hyperbolic PDEs	11
2.1.2	Berenger PML for Maxwell's equations	13
2.1.3	PML for Linearized Euler Equations	15
3	Numerical Experiments	21
3.1	Test problem	21
3.2	Numerical method	22
3.2.1	Spatial scheme	22
3.2.2	Temporal scheme	23
3.2.3	Comparison with results from [2]	23
3.3	Observation of instability in the corners of the PML	24
3.4	Applying PML on a variable coefficient problem	25
3.5	Optimizing C_x and C_y	26
3.5.1	Optimization for 2D problem	27
3.5.2	Discussion of results	28
4	Conclusions	31
	Bibliography	33

List of Figures

2.1	Aligned uniform subsonic flow	15
3.1	Computational domain with PML added.	22
3.2	Performance for the well posed PML implemented with 2nd order central differances	24
3.3	Different configurations for damping profiles in the corner regions	25
3.4	Instability in the corners	26
3.5	Simulations of different cases of variable Mach number	27
3.6	One dimensional optimization of C_x	28
3.7	Optimization for well posed PML	29

Chapter 1

Introduction

Numerical solutions of hyperbolic partial differential equations on infinite domains are usually computed on finite domains. When truncating an infinite domain to a finite domain one needs numerical boundary conditions for the far-field boundaries. Ideally these boundary conditions should prevent any non-physical reflection of outgoing waves. Further the boundary conditions should be straightforward to implement. Another demand of the boundary conditions is that they together with the problem on the truncated domain form a well posed analytical problem.

Boundary conditions of the type described above are called absorbing boundary conditions (ABCs).

The recent developments of ABCs for computational electro magnetics (CEM) have been spin offs of a technique suggested by Berenger 1994 [5]. The technique suggested by Berenger was a completely new approach on ABCs, which utterly changed the accuracy of CEM simulations. Perfectly matched layers (as Berenger named his method) have in a few years become the dominating choice for ABCs for CEM.

Attempts have been made to use the PML method suggested by Berenger for the Euler equations, for instance Hu [10]. So far the approach has not become the same success as for CEM.

Recently Abarbanel, Gottlieb and Hesthaven [2] suggested a new PML method for the linearized Euler equations. The method has the important property of being strongly well posed, a property which the previously suggested PML techniques had lacked.

The focus of this report is to present a brief outline of the history of absorbing boundary conditions and the derivation of the (by Abarbanel, Gottlieb and Hesthaven) suggested PML method. This report will also present numerical evidence for the advantages and the disadvantages of the suggested PML method.

Chapter 2

Theoretical Background

In the introduction we spoke of absorbing boundary conditions (ABCs) for hyperbolic partial differential equations (PDEs). In this chapter we present a brief historic outline of the development of ABCs for hyperbolic PDEs. We also describe a special class of ABCs known as Perfectly Matched Layer (PML). PML methods for computational electro magnetics (CEM) are currently state of the art, while PML methods for acoustic problems still a subject of research.

For a detailed discussion ABCs for hyperbolic PDEs and PML methods for CEM we refer to [12].

2.1 Absorbing boundary conditions

2.1.1 Classic analytical ABCs for hyperbolic PDEs

During the 1970's and the 1980's the research on analytical ABCs prospered and many new methods and approaches were suggested. A complete description of all of them is beyond the scope of this text and we will restrict ourselves to discussing Bayliss-Turkel radiating operators, the Engquist-Majda one way wave equation, and finally characteristic boundary conditions, before moving on to PML methods.

Bayliss-Turkel radiating operators

The idea of Bayliss and Turkel was to construct a linear partial differential operator from a weighted sum of temporal and spatial derivatives. When the operator was constructed properly it annihilated outward traveling waves leaving only a small error term behind. Bayliss and Turkel presented an operator for the three dimensional wave equation in spherical coordinates [3],[4]. For problems with spherical and cylindrical geometries their ABC worked well. However the generalization of their method to a Cartesian coordinate system became cumbersome and difficult to implement. A method which worked well for Cartesian coordinates was developed by Engquist and Majda.

Engquist Majda one way wave equation.

A PDE with solutions which describe waves that only can propagate in one direction is called a one way wave equation. Engquist and Majda realized that a one way wave equation would be ideal to use as ABC, since outward traveling waves would only be permitted to travel outward at the boundary, hence there would be no reflection at the boundary. In their classic paper [6] Engquist and Majda developed an exact one way wave-equation ABC for a Cartesian system.

They showed that for the two dimensional wave equation it was possible to construct an operator G^\pm which, when operating on the solution (U) of the two dimensional wave equation, exactly absorbed plane waves propagating toward the left or right (\pm) boundary at any angle of incidence. Thus,

$$G^\pm U = 0 \quad (2.1)$$

where

$$G^\pm \equiv D_x \pm \frac{D_t}{c} \sqrt{1 - \frac{D_y}{D_t/c}} \quad (2.2)$$

G is a so called pseudo differential operator which is nonlocal both in space and time, hence it is not possible to implement the method in a straightforward manner. This was rectified by approximating the square root with a series expansion. Engquist and Majda showed that 2nd and 4th order Taylor series expansion of the square root resulted in a strongly ill posed problem, and that an 2nd or 3rd order Padé expansion resulted in a well posed problem.

As a result of the pioneering work of Engquist and Majda a lot of similar techniques were developed. One of the more successful of them was developed by Mur [11] and is still in use as a fast but (nowadays) inaccurate method for CEM. Another set of ABCs in line with the research of Engquist and Majda was developed by Giles [7]. Giles developed ABC methods for the Euler equations which today is a commonly used ABC for the Euler equations.

Characteristic boundary conditions

ABCs for hyperbolic systems in one dimension can be derived using the theory of hyperbolic characteristics (we refer to [8] for a detailed discussion of this theory). Such boundary conditions are called characteristic boundary conditions.

To derive characteristic boundary conditions for a linear problem one makes a transformation of variables such that the coefficient matrix of the first order spatial derivative becomes diagonal. The new variables are called the characteristic variables. Each of them is associated with a characteristic curve in the space-time plane. The slope of the characteristic is determined by the corresponding diagonal element of the coefficient matrix. Information of the solution travels along the characteristics. For a problem on a, in space, bounded domain characteristics entering the domain are said to be ingoing. At a boundary point the number of

ingoing characteristics is equal to the number of boundary conditions that need to be given there. One can prevent information from entering the computational domain by setting the characteristic variables of ingoing characteristics to zero at the boundary. This is called a characteristic boundary condition.

For problems in more than one dimension we apply the theory of one dimension perpendicular to the boundary ignoring the tangential components of the impinging solution. Nonlinear problems are treated using linearization.

2.1.2 Berenger PML for Maxwell's equations

One important similarity of the above described techniques is that their performance is severely reduced at specific frequencies and angles of incidence. More or less the above described methods are optimized for normal incidence. They worked relatively well and were used in different applications during the 1970's and 1980's. In the context of CEM they are now obsolete but for other hyperbolic problems they are still used.

In the beginning of the 1990's the development of echo chambers (for electro magnetic tests) could provide experimental data far more accurate than the available numerical simulations. This renewed the research for more efficient and more accurate CEM ABCs. Since the problem of the available techniques was loss in performance at specific angles, the research was devoted to develop a technique equally efficient for all angles of incidence and frequency. In 1994 Berenger presented [5] a technique which worked equally well for all frequencies and angles. He called the technique perfectly matched layer (PML).

Instead of applying a ABC "right at" the boundary Berenger added a highly damping layer around the computational domain. To prevent reflections at the boundary between the PML and the computational domain he made them perfectly matched. Two media are said to be perfectly matched if a wave can travel across the boundary between them without any of its components being reflected. In one dimension one can compare the PML with the load of a matched transmission line. One may also compare the PML with the material in the walls of an anechoic chamber used for experimental electromagnetic tests.

The idea of a PML was simple and elegant in it's formulation, however obtaining PDEs describing a PML media was not trivial. To construct such PDEs there was a need of additional degrees of freedom to Maxwell's equations. Berenger realized that additional degrees of freedom could be introduced by splitting one of the fields (either the magnetic or the electric) into subcomponents. A short outline of his idea will be presented here, for a complete discussion we refer to Berenger's original paper [5].

We will consider the case of Maxwell's equations which describe 2D-TE po-

larized waves in vacuum. The PDEs governing the 2D-TE case are

$$\varepsilon \frac{\partial E_x}{\partial t} + \sigma_y E_x = \frac{\partial H_z}{\partial y}, \quad (2.3)$$

$$\varepsilon \frac{\partial E_y}{\partial t} + \sigma_x E_y = -\frac{\partial H_z}{\partial x}, \quad (2.4)$$

$$\mu \frac{\partial H_{zx}}{\partial t} + \sigma_x^* H_{zx} = -\frac{\partial E_y}{\partial x}, \quad (2.5)$$

$$\mu \frac{\partial H_{zy}}{\partial t} + \sigma_y^* H_{zy} = \frac{\partial E_x}{\partial y}. \quad (2.6)$$

Here the splitting $H_z = H_{zx} + H_{zy}$ has been introduced. σ_x, σ_y are the electric conductivities and σ_x^*, σ_y^* the magnetic losses. When (2.3-2.6) is transformed to the time harmonic plane where they become

$$j\omega\varepsilon \left(1 + \frac{\sigma_y}{j\omega\varepsilon}\right) \hat{E}_x = \frac{\partial}{\partial y} (\hat{H}_{zx} + \hat{H}_{zy}), \quad (2.7)$$

$$j\omega\varepsilon \left(1 + \frac{\sigma_x}{j\omega\varepsilon}\right) \hat{E}_y = -\frac{\partial}{\partial x} (\hat{H}_{zx} + \hat{H}_{zy}), \quad (2.8)$$

$$j\omega\mu \left(1 + \frac{\sigma_x^*}{j\omega\mu}\right) \hat{H}_{zx} = -\frac{\partial \hat{E}_y}{\partial x}, \quad (2.9)$$

$$j\omega\mu \left(1 + \frac{\sigma_y^*}{j\omega\mu}\right) \hat{H}_{zy} = \frac{\partial \hat{E}_x}{\partial y}. \quad (2.10)$$

If we differentiate (2.7) with respect to y and (2.8) with respect to x and then substitute $\frac{\partial \hat{E}_x}{\partial y}$ and $\frac{\partial \hat{E}_y}{\partial x}$ into (2.9), (2.10) we obtain the wave equation (2.11).

$$\frac{1}{s_x^*} \frac{\partial}{\partial x} \frac{1}{s_x} \frac{\partial}{\partial x} \hat{H}_z + \frac{1}{s_y^*} \frac{\partial}{\partial y} \frac{1}{s_y} \frac{\partial}{\partial y} \hat{H}_z + \omega^2 \mu \varepsilon \hat{H}_z = 0, \quad (2.11)$$

where we have used.

$$s_w = \left(1 + \frac{\sigma_w}{j\omega\varepsilon}\right), \quad s_w^* = \left(1 + \frac{\sigma_w^*}{j\omega\varepsilon}\right), \quad w = x, y.$$

The wave equation (2.11) supports superposition of solutions of the form

$$\hat{H}_z = H_0 \tau e^{-j\sqrt{s_x s_x^*} \beta_x x - j\sqrt{s_y s_y^*} \beta_y y}.$$

By analysis of the dispersion relation of (2.11) one derives conditions for the transmission coefficient τ . The condition $\tau = 1$ is accomplished by setting $\frac{\sigma_z}{\varepsilon} = \frac{\sigma_z^*}{\mu}$, $z = x, y$. Since $\sigma_z, \sigma_z^*, \varepsilon$ and μ do not depend on frequency or angle, the layers are perfectly matched for all frequencies and angles.

However the system of PDEs describing the PML suggested by Berenger was shown by Abarbanel and Gottlieb [1] to be only weakly well posed i.e. the system of PDEs may become ill posed under some perturbations. An example of a perturbation which renders an ill posed system of PDEs can be found in [1].

2.1.3 PML for Linearized Euler Equations

We begin by formulating the linearized Euler equations of gas-dynamics. Since there is more than one way of formulating the Euler equations, we have chosen to formulate them in line with [2].

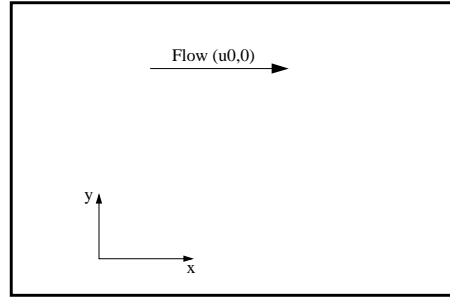


Figure 2.1. Aligned uniform subsonic flow

Linearized Euler equations

Consider waves in a two-dimensional uniform, isentropic, subsonic flow, $(u_0, 0)$ (shown in figure 2.1) of a compressible fluid with constant density ρ_0 . For small perturbations in the density (ρ) and the velocity components (u, v) we may linearize and nondimensionalize the equations of gas-dynamics so that we get the linearized Euler equations

$$\frac{\partial \rho}{\partial t} + M \frac{\partial \rho}{\partial x} + \frac{\partial u}{\partial x} + \frac{\partial v}{\partial y} = 0, \quad (2.12)$$

$$\frac{\partial u}{\partial t} + M \frac{\partial u}{\partial x} + \frac{\partial \rho}{\partial x} = 0, \quad (2.13)$$

$$\frac{\partial v}{\partial t} + M \frac{\partial v}{\partial x} + \frac{\partial \rho}{\partial y} = 0. \quad (2.14)$$

M is the Mach number, which is restricted to $M \in [0, 1]$.

Note that by setting $M = 0$ and $v = -E_x, u = E_y, \rho = H_z$, in (2.12-2.14) we recover Maxwell's equations describing the 2D-TM mode, for which we may apply CEM PML methods directly.

Split field PML-method

In [10] Hu presented a set of PDEs describing a PML for the linearized Euler equations. The set of equations were derived in the context of Berenger split-field formalism.

Hu started with a slightly different formulation of the linearized Euler equations, which also contain the pressure (p),

$$\frac{\partial u}{\partial t} + M \frac{\partial u}{\partial x} = -\frac{\partial p}{\partial x}, \quad (2.15)$$

$$\frac{\partial v}{\partial t} + M \frac{\partial v}{\partial x} = -\frac{\partial p}{\partial y}, \quad (2.16)$$

$$\frac{\partial p}{\partial t} + M \frac{\partial p}{\partial x} = -\left(\frac{\partial u}{\partial x} + \frac{\partial v}{\partial y}\right), \quad (2.17)$$

$$\frac{\partial \rho}{\partial t} + M \frac{\partial \rho}{\partial x} = -\left(\frac{\partial u}{\partial x} + \frac{\partial v}{\partial y}\right). \quad (2.18)$$

For (2.15-2.18) Hu introduced the splitting $u = u_1 + u_2$, $v = v_1 + v_2$, $p = p_1 + p_2$, $\rho = \rho_1 + \rho_2$ and added damping profiles σ_x , σ_y . This resulted in system of eight equations, which supports plane wave solutions of the form

$$\begin{aligned} [u_1, u_2, v_1, v_2, \\ p_1, p_2, \rho_1, \rho_2] &= [u_{10}, u_{20}, v_{10}, v_{20}, \\ & p_{10}, p_{20}, \rho_{10}, \rho_{20}] e^{j(k_x x + k_y y - \omega t)}. \end{aligned} \quad (2.19)$$

Inserting (2.19) into the split field formulation of (2.15-2.18) yields

$$(\omega + j\sigma_x)u_{10} = k_x(p_{10} + p_{20}), \quad (2.20)$$

$$(\omega + j\sigma_x)u_{20} = k_x M(u_{10} + u_{20}), \quad (2.21)$$

$$(\omega + j\sigma_y)v_{10} = k_y(p_{10} + p_{20}), \quad (2.22)$$

$$(\omega + j\sigma_x)v_{20} = k_x M(v_{10} + v_{20}), \quad (2.23)$$

$$(\omega + j\sigma_x)p_{10} = k_x(u_{10} + u_{20}) + k_x M(p_{10} + p_{20}), \quad (2.24)$$

$$(\omega + j\sigma_y)p_{20} = k_y(v_{10} + v_{20}), \quad (2.25)$$

$$(\omega + j\sigma_x)\rho_{10} = k_x(u_{10} + u_{20}) + k_x M(\rho_{10} + \rho_{20}), \quad (2.26)$$

$$(\omega + j\sigma_y)\rho_{20} = k_y(v_{10} + v_{20}), \quad (2.27)$$

which support sound- and vorticity-waves. By analyzing the reflection and transmission between two PML Hu derived conditions for matching between them at all angles and frequencies.

The numerical results Hu presented were promising, however he reported that he had to apply a low-pass filter to avoid instability inside the PML. The explanation for the instabilities has been given by Hesthaven [9]. He showed (similar to the case of Berengers PML) that the instability is a result of the system only being weakly well posed. It can become ill posed under low order perturbations. This is a major drawback for Hu's split field technique.

Well posed PML method

Recently a well posed PML method for the linearized Euler equations was suggested by Abarbanel, Gottlieb and Hesthaven [2]. They developed it using the same

mathematical framework as for the derivation of a well posed PML for Maxwell's equations, see [1].

The PDEs for which a PML is to be developed are (2.12- 2.14). For the case $M=0$ solutions to this system may be expressed as superpositions of plane waves of the form

$$\begin{pmatrix} \rho \\ u \\ v \end{pmatrix} = \begin{pmatrix} 1 \\ \alpha \\ \beta \end{pmatrix} e^{iw(t-\alpha x-\beta y)}, \quad (2.28)$$

with the standard dispersion relation $\alpha^2 + \beta^2 = 1$. For this case it is straightforward to use the techniques developed for electro magnetics.

When $M \neq 0$ the dispersion relations become difficult to express. A way to circumvent this problem is to introduce a variable transformation such that the dispersion relation has the above simple form. The transformation suggested by Abarbanel, Gottlieb and Hesthaven is

$$\xi = x, \quad (2.29)$$

$$\eta = \sqrt{1 - M^2}y = \gamma y, \quad (2.30)$$

$$\tau = Mx + \gamma^2 t. \quad (2.31)$$

In the stretched space (ξ, η, τ) the linearized Euler equations (2.12- 2.14) become

$$\frac{\partial v}{\partial \tau} + M \frac{\partial v}{\partial \xi} + \gamma \frac{\partial \rho}{\partial \eta} = 0, \quad (2.32)$$

$$\frac{\partial u}{\partial \tau} + \frac{\partial \rho}{\partial \xi} - \frac{M}{\gamma} \frac{\partial v}{\partial \eta} = 0, \quad (2.33)$$

$$\frac{\partial \rho}{\partial \tau} + \frac{\partial u}{\partial \xi} + \frac{1}{\gamma} \frac{\partial v}{\partial \eta} = 0. \quad (2.34)$$

Solutions to (2.32-2.34) may be expressed as superposition of waves of the form

$$\begin{pmatrix} \rho \\ u \\ v \end{pmatrix} = \begin{pmatrix} q_1 \\ q_2 \\ q_3 \end{pmatrix} e^{iw(\tau - B\eta - \lambda\xi)}. \quad (2.35)$$

Here λ must be one of the following eigenvalues

$$\lambda_0 = 1/M, \quad (2.36)$$

$$\lambda_1 = \sqrt{1 - B^2} \equiv A, \quad (2.37)$$

$$\lambda_2 = -\sqrt{1 - B^2} = -A. \quad (2.38)$$

The three corresponding eigenvectors are

$$\mathbf{q}_0 = \begin{pmatrix} M \\ -\frac{M^2 B}{\gamma} \\ 0 \end{pmatrix}, \quad (2.39)$$

$$\mathbf{q}_1 = \begin{pmatrix} B\gamma \\ A - M \\ 1 - MA \end{pmatrix}, \quad (2.40)$$

$$\mathbf{q}_2 = \begin{pmatrix} B\gamma \\ -A - M \\ 1 + MA \end{pmatrix}. \quad (2.41)$$

We begin by describing the procedure to construct the PML-equations for the layer $-L_x - \delta_x \leq x \leq -L_x$ i.e. the leftmost layer in figure 3.1. For this layer the eigenvalue $\lambda_2 = -A \leq 0$ is the relevant one. It corresponds to solution moving to the left. Abarbanel, Gottlieb and Hesthaven assumed the existence of a solution expressed as a superposition of waves of the form

$$\begin{pmatrix} v \\ u \\ \rho \end{pmatrix} = \begin{pmatrix} (1+g)B\gamma \\ -(1+f)(A+M) \\ (1+h)(1+MA) \end{pmatrix} e^{i\omega(\tau+A\xi-B\eta)} e^{-A \int_{\xi \leq 0}^0 \sigma_x(z) dz}. \quad (2.42)$$

By inserting (2.42) into (2.32-2.34) they got three relations from which they determined the functions f , g and h . Then they added three variables Q_x , R_x , P_x , defined in such a way that it is possible to eliminate all dependence of A , B , ω . The same procedure was done for the other layers rendering the set of equations valid for the

whole PML. After inverting the transformation (2.29-2.31) the equations are

$$\begin{aligned}
\frac{\partial v}{\partial t} + M \frac{\partial v}{\partial x} + \frac{\partial \rho}{\partial y} &= -\sigma_x v + 2\sigma_x Q_x + \sigma_x^2 R_x + M \sigma_x' P_x + 2\sigma_y Q_y \\
&\quad + \sigma_y^2 R_y + \sigma_y' P_y - \varepsilon_x v + 2\mu_y Q_y, \\
\frac{\partial u}{\partial t} + M \frac{\partial u}{\partial x} + \frac{\partial \rho}{\partial x} &= -\sigma_x u - \sigma_x M \rho - \mu_y u, \\
\frac{\partial \rho}{\partial t} + M \frac{\partial \rho}{\partial x} + \frac{\partial u}{\partial x} + \frac{\partial v}{\partial y} &= -\sigma_x \rho - \sigma_x M u - \mu_y \rho, \\
\frac{\partial Q_x}{\partial t} &= -\gamma^2 \frac{\partial \rho}{\partial y}, \\
\frac{\partial Q_y}{\partial t} &= \gamma^2 \left[\frac{\partial \rho}{\partial y} - 2\sigma_y Q_y - \sigma_y^2 R_y - \sigma_y' P_y + \sigma_x v \right. \\
&\quad \left. - 2\sigma_x Q_x - \sigma_x^2 R_x - M \sigma_x' P_x + \mu_x v - 2\mu_y Q_y \right], \\
\frac{\partial P_x}{\partial t} &= \gamma^2 [v - \sigma_x P_x - \varepsilon_x P_x], \\
\frac{\partial P_y}{\partial t} &= \gamma^2 [\rho - \sigma_y P_y], \\
\frac{\partial R_x}{\partial t} &= \gamma^2 [Q_x - \mu_x R_x], \\
\frac{\partial R_y}{\partial t} &= \gamma^2 [Q_y - \mu_y R_y].
\end{aligned} \tag{2.43}$$

Following [2] extra terms with coefficients $\varepsilon_x(x)$, $\mu_x(x)$, $\mu_y(y)$ are introduced in (2.43). These terms are motivated by an analysis of the corresponding equations without the spatial derivatives in each of the layers (the x-layer is the layer perpendicular to the x-axis). Here the analysis is presented only for the x-layer. We can ignore ρ and v since they are decoupled. This results in a system of ODEs

$$\begin{aligned}
\frac{\partial v}{\partial t} &= -\sigma_x v + 2\sigma_x Q_x + \sigma_x^2 R_x + M \sigma_x' P_x, \\
\frac{\partial Q_x}{\partial t} &= 0, \quad \frac{\partial P_x}{\partial t} = \gamma^2 (v - \sigma_x P_x), \quad \frac{\partial R_x}{\partial t} = \gamma^2 Q_x.
\end{aligned} \tag{2.44}$$

The eigenvalues of 2.44 are determined in [2]. Abarbanel, Gottlieb and Hesthaven found that there was a need to add the profiles ε_x and μ_x to the set of ODEs (2.44) in order shift the eigenvalues into the left half of the complex plane. For the y-layer a similar analysis was done. According to [2] the following conditions should be fulfilled,

$$\begin{aligned}
\varepsilon_x &\geq \sqrt{|M \sigma_x'|}, \\
\mu_x &\geq 0, \\
\mu_y &\geq 0.
\end{aligned}$$

The damping profiles are functions of the depth of the PML starting on zero and increasing to a maximum value. The damping should be as strong as possible. However the damping profiles may not be too strong because then they cause

reflections at the boundary due to the discretization of the function describing the damping parameter. The solution is to choose the damping parameters to be a gradually increasing function inside the PML. Usually one uses a polynomial of degree 3-5 which starts at 0 at the interface and rises to a maximum value at the end of the PML. The degree of the polynomial is chosen empirically.

Chapter 3

Numerical Experiments

3.1 Test problem

The test problem is adopted from [2]. It is a standard problem from aero-acoustics and there exists an analytical solution. The numerical solution was not compared with the analytical solution but with a reference solution for the same problem on a larger domain. The size of the reference domain is chosen such that no waves have time to travel back to the original computational domain. This type of comparison provides a true estimate of the performance of the PML. The geometry of the problem is shown in figure 3.1. In the inner domain, the PDEs (2.12-2.14) are solved, and in the outer domain the PDEs (2.43)

Forcing

In the inner domain ρ , u and v are subjected to the continuous forcing

$$\begin{aligned}\rho^f(x, y, t) &= e^{-\frac{(\ln 2)(x-x_a)^2+(y-y_a)^2}{\delta_a^2}} \sin\left(\frac{\pi t}{10}\right), \\ u^f(x, y, t) &= 0.05(y-y_b)e^{-\frac{(\ln 2)(x-x_b)^2+(y-y_b)^2}{\delta_b^2}} \sin\left(\frac{\pi t}{10}\right), \\ v^f(x, y, t) &= -0.05(x-x_b)e^{-\frac{(\ln 2)(x-x_b)^2+(y-y_b)^2}{\delta_b^2}} \sin\left(\frac{\pi t}{10}\right),\end{aligned}\quad (3.1)$$

where (x_a, y_a) is the center of the sound source, which has the width δ_a , (x_b, y_b) is center of the vorticity source with width δ_b . The centers were chosen as $(x_a, y_a) = (-25, 0)$, $(x_b, y_b) = (25, 0)$, $\delta_a = 3$, $\delta_b = 4$.

The computational domain is bounded by $|x| \leq L_x$, $|y| \leq L_y$, for our tests we choose $L_x = L_y = 50$.

PML

The PML layer is added to the computational domain according to figure 3.1.

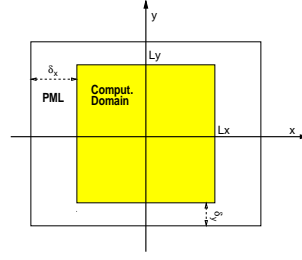


Figure 3.1. Computational domain with PML added.

The layer-thickness is represented by δ_x and δ_y . The profile of the damping parameters σ_x and σ_y are described by

$$\sigma_x(x) = \begin{cases} 0, & |x| \leq L_x \\ C_x \left(\frac{|x-L_x|}{\delta_x} \right)^n, & L_x \leq |x| \leq L_x + \delta_x \end{cases}$$

$$\sigma_y(y) = \begin{cases} 0, & |y| \leq L_y \\ C_y \left(\frac{|y-L_y|}{\delta_y} \right)^n, & L_y \leq |y| \leq L_y + \delta_y \end{cases}$$

As discussed earlier we note that it is important that the value of C_x and C_y is high enough to damp outgoing waves efficiently, still it may not be too high, since the discretization of σ generates reflections for the numerical solution. If σ grow too fast (i.e. n must not be chosen too high) it will limit the efficiency of the PML.

The parameters $C_{x,y}$, $\delta_{x,y}$ and n are to be chosen in such a way that the performance of the PML is optimal. We have studied different choices of the parameters $C_{x,y}$ and $\delta_{x,y}$ but kept n to 4 for all tests. The PML is terminated with characteristic boundary conditions.

3.2 Numerical method

3.2.1 Spatial scheme

The problem was discretized in space with 2nd order central differences (in [2] 4th order central differences, were used). The reason for choosing this low order method is it's simplicity to implement. For more thorough studies one needs to use a higher order method. The spatial discretisation on the computational domain was chosen as $\Delta x = \Delta y = 1$.

Characteristic Boundary condition

We end the spatial scheme with characteristic boundary conditions i.e we put incoming characteristic variables to zero. For the outgoing characteristic variables

we need a numerical condition. We chose to extrapolate the outgoing characteristic variables linearly. This means that if s is a characteristic outgoing variable at the left boundary x_0 we have $s_0 = 2s_1 - s_{-2}$. Here $s_i \approx s(x_0 + i\Delta x)$.

For our problem the characteristic boundary conditions expressed in original variables become,

$$\begin{aligned}
v_{i,-N_y} &= \frac{1}{2}(2v_{i,-N_y+1} - 2\rho_{i,-N_y+1} - v_{i,-N_y+2} + \rho_{i,-N_y+2}), \\
v_{N_x,j} &= 2v_{N_x-1,j} - v_{N_x-2,j} \quad v_{-N_x,j} = 0, \\
v_{i,N_y} &= \frac{1}{2}(2v_{i,N_y-1} + 2\rho_{i,N_y-1} - v_{i,N_y-2} - \rho_{i,N_y-2}), \\
u_{i,-N_y} &= 2u_{i,-N_y+1} - u_{i,-N_y+2}, \quad u_{i,N_y} = 2u_{i,N_y-1} - u_{i,N_y-2}, \\
u_{-N_x,j} &= \frac{1}{2}(2u_{-N_x+1,j} - 2\rho_{-N_x+1,j} - u_{-N_x+2,j} + \rho_{-N_x+2,j}), \\
u_{N_x,j} &= \frac{1}{2}(2u_{N_x-1,j} + 2\rho_{N_x-1,j} - u_{N_x-2,j} - \rho_{N_x-2,j}), \\
\rho_{i,-N_y} &= \frac{1}{2}(2\rho_{i,-N_y+1} - 2v_{i,-N_y+1} + v_{i,-N_y+2} - \rho_{i,-N_y+2}), \\
\rho_{i,N_y} &= \frac{1}{2}(2v_{i,N_y-1} + 2\rho_{i,N_y-1} - v_{i,N_y-2} - \rho_{i,N_y-2}), \\
\rho_{-N_x,j} &= \frac{1}{2}(2\rho_{-N_x+1,j} - 2u_{-N_x+1,j} + u_{-N_x+2,j} - \rho_{N_x+2,j}), \\
\rho_{N_x,j} &= \frac{1}{2}(2u_{N_x-1,j} + 2\rho_{N_x-1,j} - u_{N_x-2,j} - \rho_{N_x-2,j}).
\end{aligned}$$

Where $v_{i,j} \approx v(i\Delta x, j\Delta y)$ and $i = -N_x..0..N_x$, $j = -N_y..0..N_y$ where $N_x = L_x/\Delta x$, $N_y = L_y/\Delta y$, etc.

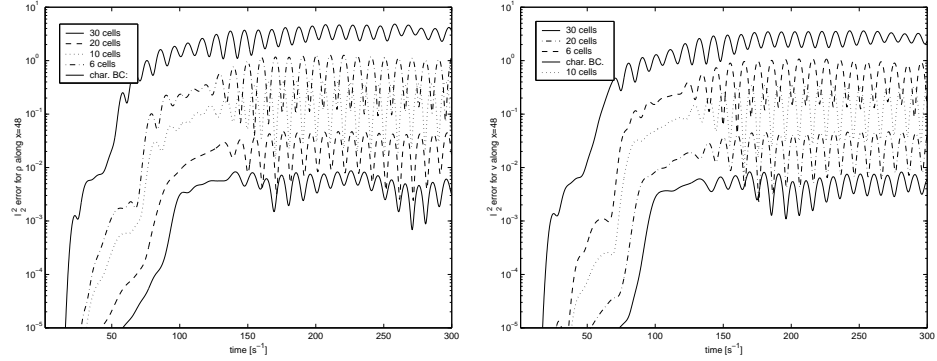
3.2.2 Temporal scheme

The problem was advanced forward in time using the classic 4th order Runge Kutta method. To maintain stability we used a time step $\Delta t \leq 0.5$ (with $\Delta x = \Delta y = 1$, $C_x = C_y = 1$, $M = 0.5$). The stability limit was established with numerical experiments. The stability limit is sharpened if the PML is provided with stronger damping terms i.e higher C_x , C_y .

3.2.3 Comparison with results from [2]

As a measure of the performance of the PML we chose (in resemblance with [2]) the l_2^2 error along the line $x = 48$, $|y| \leq 48$. A comparison with the results from [2] shows that the problem discretized with 2nd order central differences in principle and form gives the same results. The magnitude of the error is two orders of magnitude larger. The relative difference between computations from computations with varying of PML thickness is the same.

The figures 3.2(a) and 3.2(b) show the error along the line $x=48$ for different choices of PML thickness (for the 2nd order scheme). For this computation we



(a) The error along $x=48$ for ρ for different layer thickness for the well posed PML

(b) The error along $x=48$ for v for different layer thickness for the well posed PML

Figure 3.2. Performance for the well posed PML implemented with 2nd order central differences

chose $C_x = C_y = 1$. We note that the improvement in performance between characteristic boundary conditions and a 30-cell thick PML is about 4 orders of magnitude.

3.3 Observation of instability in the corners of the PML

When we discussed the derivation of the PML equations we noted that the stability profiles ϵ_x , μ_x , μ_y were derived separately for the x-layer and the y-layer. The profiles ϵ_x , μ_x , μ_y are a necessary but not sufficient condition to guarantee us stable solutions for the configurations of the PML described in figures (3.3(b)-3.3(d)), since there is no overlap of the layers for those configurations. For the configuration in figure 3.3(a) there is no guarantee at all for stable solutions since no analysis have been done for the coupled set of PDEs in the corners.

For the case when both C_x and C_y are nonzero in the corner regions we experienced instability originating in the corners. In figure 3.4(a) we see that the solution grows unbounded at time approximately 125. In figure 3.4(b) we see how the growth originates in the corner regions. The solution exploded at an earlier time if C_x and C_y was increased. To avoid this instability we have chosen the configuration of the PML according to figure 3.3(c) which gave the PML the best performance.

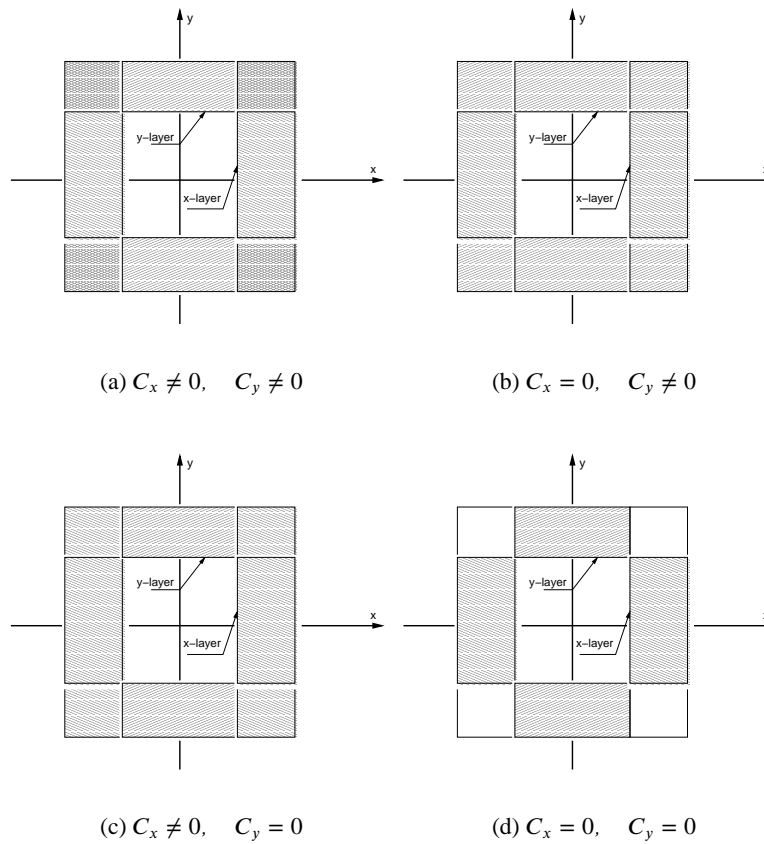


Figure 3.3. Different configurations for damping profiles in the corner regions

3.4 Applying PML on a variable coefficient problem

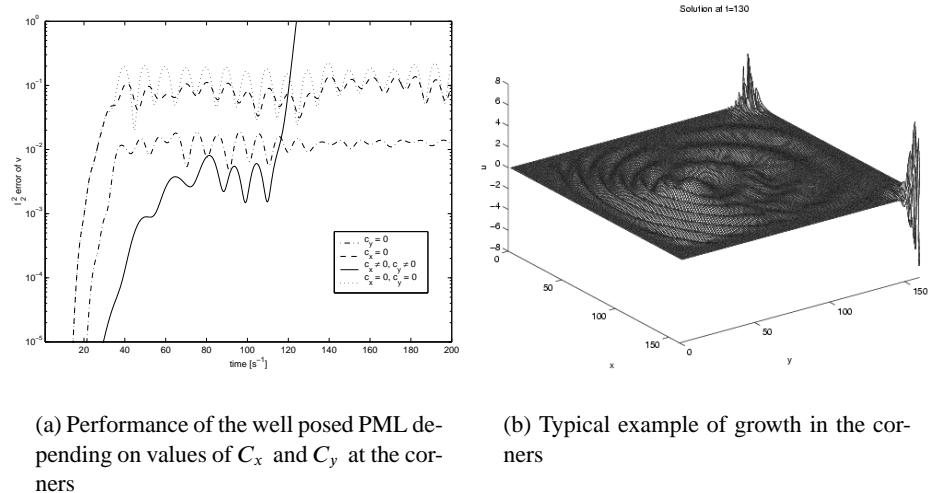
To decide whether a ABC technique derived for constant Mach number is practically useful it is important to test it's performance on a problem with variable Mach number i.e. $M = M(x, y)$. To test the suggested PML we computed solutions for two flows with varying Mach number. We varied the Mach Number according to the function

$$M = M(z) = e^{\frac{-z^2}{10^2}} \quad (3.2)$$

where z is either x or y .

Subsonic jet

The first problem is supposed to be a simulation of a subsonic jet. The Mach number is described by equation 3.2 with $z = x$, which means higher Mach



(a) Performance of the well posed PML depending on values of C_x and C_y at the corners

(b) Typical example of growth in the corners

Figure 3.4. Instability in the corners

number in the middle of the flow and lower towards the y-layers. The result can be seen in figure 3.5(a) and figure 3.5(b).

Nozzle

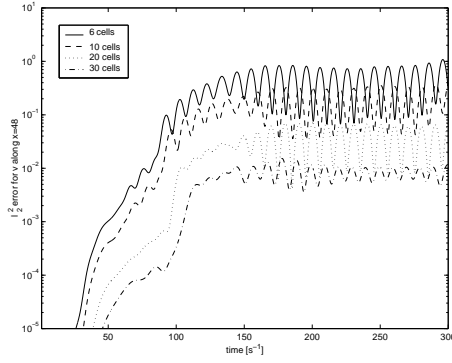
In the second problem the Mach number varies in the streamwise direction as in a slim nozzle. The Mach number is described by equation 3.2 with $z = y$, which means higher Mach number in the middle of the flow and lower towards the x-layers. The result can be seen in figure 3.5(c) and figure 3.5(d).

Results

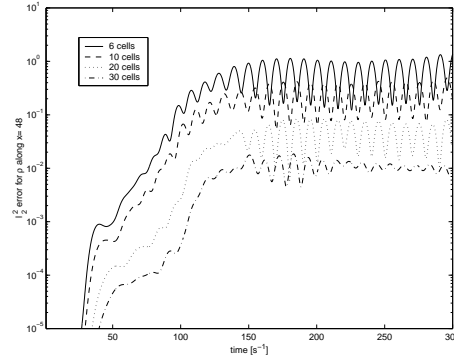
The spatial variation of the Mach number does not seem to effect the performance of the PML and a realistic assumption is that this method may be applied without to much constrains on problems with variable Mach number.

3.5 Optimizing C_x and C_y

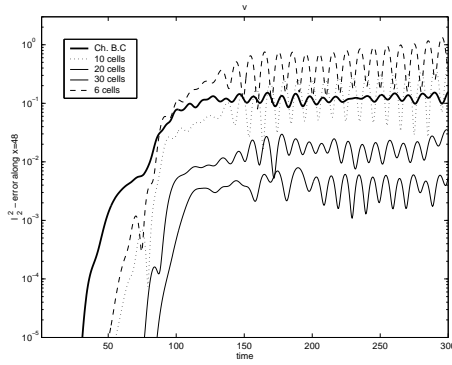
Since it is pointed out in [2] that no optimization of the parameters C_x and C_y was performed we attempted to optimize the value of those parameters. The first step was to analyze the one dimensional case governed by the PDEs describing the x-layer. For the one dimensional case we found that the optimal value of C_x was quite close to 1 but was shifted upwards for thinner PML. The results can be seen in figure 3.5. Note that the PML is more efficient than characteristic boundary



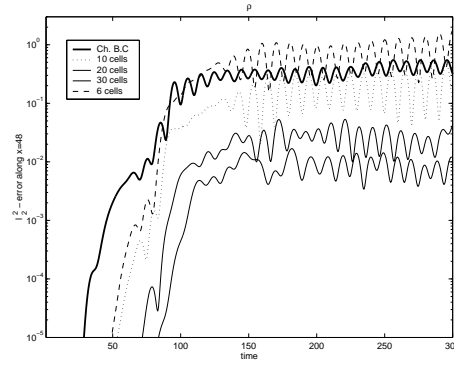
(a) Error along $x=48$ for v for a simulated subsonic jet



(b) Error along $x=48$ for ρ for a simulated subsonic jet



(c) Error along $x=48$ for v for a simulated slim nozzle



(d) Error along $x=48$ for ρ for a simulated slim nozzle

Figure 3.5. Simulations of different cases of variable Mach number

conditions only for PMLs thicker than 20 cells. This leads us to conclude that for the one dimensional problem the profit of using PML is rather limited.

3.5.1 Optimization for 2D problem

In order to compare the one dimensional optimization with a two dimensional optimization we computed solutions where we varied C_x and C_y between 0-1 for a 15 cell PML. The results can be seen in figures (3.7(d))-3.7(e)).

For the two dimensional problem we expected to find the same type of minima at $C_x = C_y \approx 1$ as for the one dimensional problem, however the results show that the optimal performance of the 15 cell PML is for $C_x=C_y=0$. Since $C_x=C_y=0$

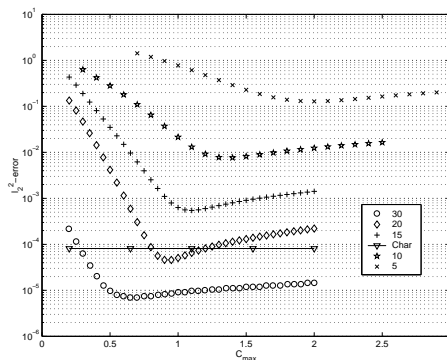


Figure 3.6. One dimensional optimization of C_x

corresponds to adding 15 “empty” cells and terminating them with characteristic boundary conditions the result was a bit unexpected. Calculations with a 30 cell PML were performed. For this test the PML was seen to be more effective than characteristic boundary conditions. This can be seen in figure (3.7(b)).

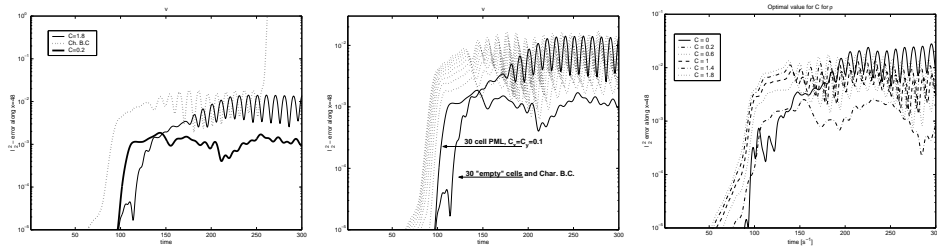
However if we choose to compare the performance of the PML with the case with “empty” cells terminated with characteristic boundary conditions we conclude the advantage using PML will not be obvious. Especially not taken in to account that the PML method requires three times more computer memory storage for the additional layer than if we only solve the original problem on a equally large domain terminated with characteristic boundary conditions. Note that by only studying the results in figure 3.2(a) and [2] the impression one gets is that the method is very good.

Another case of instability

We have also observed that when we make C_x and C_y larger without reducing the time-step we find a limit where the solutions grow unbounded (note that this is for the case when the profiles of the damping parameters do not overlap in the corners). An example of the instability is provided in figure 3.7(a). From experiments we conclude that the stability limit depends on C_x and C_y .

3.5.2 Discussion of results

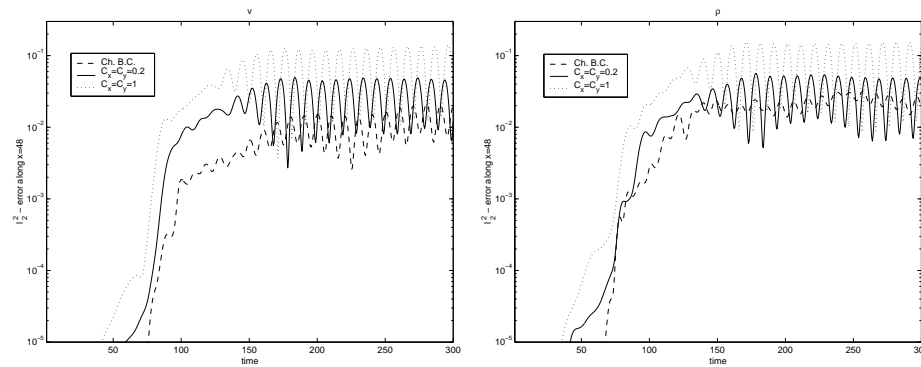
To explain the performance of the PML we need to recall the two mechanisms of a PML, matching and damping. If the matching is not perfect there will be reflections at the transition between the PML and the computational domain. If the damping is too low the boundary condition at the outermost boundary will still be limiting the performance of the PML. A similar decrease in performance will be noted if the damping profiles are increasing faster than the method is able to resolve (which may be the case when working with a low order method).



(a) Variation of C for a 30 cell PML. For $C=2$ we experience instability

(b) Variation of C for a 30 cell PML. Note that the PML is more efficient than Ch. B.C for $C=0.2$

(c) Variation of C for a 30 cell PML



(d) Variation of C for a 15 cell PML. The curves describe the error of v along $x=48$. Only three values for C has been displayed for clarity

(e) Variation of C for a 15 cell PML. The curves describe the error of ρ along $x=48$. Only three values for C has been displayed for clarity

Figure 3.7. Optimization for well posed PML

The introduction of the stabilizing profiles ε_x , μ_x and μ_y possibly destroys the perfect matching of the PML. This could be one explanation for the poor performance of the PML. Another cause could be that the low order scheme which we used limits the efficiency of the PML by not properly resolving the variations of the solution in the damping regions.

Chapter 4

Conclusions

The PML method suggested by Abarbanel, Gottlieb and Hesthaven in [2] have been examined with numerical experiments which have revealed some advantages and some disadvantages of the method. We would like to emphasize that the not so positive results from numerical experiments that we have presented can be seen as an agenda for future theoretical work, which need to be done in order to make the suggested PML method robust and more efficient.

Variable coefficients

The suggested PML method has been applied on problems with spatially varying Mach number. The performance of the PML is insensitive to these spatial variations. At this state we believe that the suggested PML method may be applied to problems with variations of the Mach number without any particular modifications or restrictions.

Stability properties

On the basis of the instabilities observed in the corners and the instabilities observed when the damping strength is increased we conclude that the PML changes the stability properties of the Euler equations. The stability properties are needed to be better understood for the corners and for the PML.

Higher order method

In order to accurately simulate wave phenomena one should in general use a higher order method. Therefore future work should be done using a, at least, 4th order discretization. Also at this state we cannot exclude that the lack of performance of the suggested PML method, partly is due to the use of a lower order method.

Acknowledgments

I would like to thank my supervisor Gunilla Kreiss for excellent supervision of this Master's project.

Bibliography

1. S. Abarbanel and D. Gottlieb. A mathematical analysis of the pml method. *J. Comput. Phys.*, 134:357, 1997.
2. S. Abarbanel, D. Gottlieb, and J.S Hesthaven. Well-posed perfectly matched layers for advective acoustics. *Journal of Computational Physics*, 154:266–283, 1999.
3. A. Bayliss, M. Ginzburger, and E. Turkel. Boundary conditions for the numerical solution of elliptic equations in exterior regions. *SIAM Journal of Applied Mathematics*, 42:430–451, 1982.
4. A. Bayliss and E. Turkel. Radiation boundary conditions for wave-like equations. *Comm. Pure Appl. Math.*, 33:707, 1980.
5. J. P. Brernger. A perfectly matched layer for the absorption of electromagnetic waves. *Journal of Computational Physics*, 114:185, 1994.
6. B. Engquist and A. Majda. Absorbing boundary conditions for the numerical simulation of waves. *Math. Comp.*, 31:629, 1977.
7. M. Giles. Non-reflecting boundary conditions for the euler equations. *CFDL-TR*, 1988.
8. Gustafsson, Kreiss, and Olinger. *Time dependent problems and difference methods*. Wiley, 1995.
9. J.S. Hesthaven. On the analysis and construction of perfectly matched layers for the linearized euler equations. *Journal of computational Physics*, 142:129–147, 1998.
10. F. Q. Hu. On absorbing boundary conditions for linearized euler equations by a perfectly matched layer. *Journal of Computational Physics*, 129:201–209, 1996.
11. G. Mur. Absorbing boundary conditions for the finite-difference approximation of the time-domain electromagnetic field equations. *IEEE Trans. Electromagnetic Compatibility*, 23:377–382, 1981.
12. Allen Taflove. *Computational electrodynamics: the finite-difference time-domain method*. Artech House, 2nd edition, 2000.